Limits in determining permeability from on-the-fly uCPT sounding

D. ELSWORTH* and D. S. LEE

Limits are defined for the transition from partially drained to undrained penetration during uCPT testing. These limits prescribe the range of cone metrics for which coefficient of permeability magnitudes may be recovered from peak pore pressure data, on the fly. The transition from partially drained to undrained behaviour is defined through the traditional non-dimensional metrics of cone resistance Q_t, sleeve friction F_r and pore pressure ratio B_q, together with the undrained shear strength S_u, normalised by shear modulus G and in situ effective stress, σ'_{v0}. For plausible ranges of S_u/σ'_{v0} and G/S_u, the lower bound for transition from partial drainage is defined by the uCPT metric products and ratios of $B_q Q_t = 1.2$, $Q_t F_r = 0.3$, and $B_q/F_r = 4$, with the first and last proving the best determinants of drainage condition. Standard (2 cm/s and 10 cm^2 face area) uCPT data together with independently measured permeabilities identify the transition from partially drained to undrained conditions at permeability magnitudes of the order of 10^{-5} m/s. These results are used to define limits of partial drainage where peak tip pore pressures may be used to recover in situ permeability profiles. For conditions of partial drainage, a non-dimensional permeability K_D is defined independently in terms of cone metrics as $K_D = 1/B_q Q_t$ (with $B_q Q_t < 1.2$), enabling permeability to be recovered during standard penetration for $K > 10^{-5}$ m/s. Where undrained data are excluded, non-dimensional permeability K_D is optimally defined as $K_D = 0.62/(B_q Q_t)^{1.6}$.

KEYWORDS: groundwater; in situ testing; permeability; pore pressures; site investigation; soil classification

Des limites sont définies pour la transition de la pénétration partiellement drainée à la pénétration non drainée au cours d'essais uCPT. Ces limites prescrivent la gamme des mesures coniques pour lesquelles on peut obtenir un coefficient de magnitudes de perméabilité à partir de données de pression de pores de pointe, à la volée. La transition du comportement partiellement drainé au comportement non drainé est définie par le biais de la mesure non dimensionnelle traditionnelle de la résistance conique Q_t, la friction de la bague F_r et le ratio de pression de pore B_q, ainsi que la résistance au cisaillement non drainé S_u, normalisée par le module d'élasticité G et la tension efficace σ'_{v0}. Pour des plages plausibles de S_u σ'_{v0} et G/S_u, la limite inférieure pour la transition depuis le drainage partie est définie par les produits métriques uCPT et les ratios de $B_q Q_t = 1.2$, $Q_t F_r = 0.3$, et $B_q/F_r = 4$, le premier et le dernier s'avérant être les meilleurs déterminants du drainage. Des données uCPT standards (2 cm/s et superficie de la face de 10 cm^2), ainsi que des perméabilités mesurées indépendamment, identifient la transition des conditions partiellement drainée à non drainée avec des magnitudes de perméabilité de l'ordre de 10^{-5} m/s. Ces résultats sont utilisés pour définir les limites d'un drainage partiel où les pressions de pore de pointe peuvent être utilisées pour obtenir des profils de perméabilité in situ. Dans les situations de drainage partiel, on définit une perméabilité non dimensionnelle K_D indépendamment sur le plan de la mesure des cônes de la façon suivante : $K_D = 1/B_q Q_t$ ($B_q Q_t < 1,2$), ce qui permet d'obtenir la perméabilité au cours d'une pénétration standard pour k $> 10^{-5}$ m/s. Lorsqu'on exclut des données non drainées, la définition optimale de la perméabilité non dimensionnelle K_D est $K_D = 0,62/(B_q Q_t)1.6$.

INTRODUCTION

Piezocone sounding (uCPT) is a rapid, minimally invasive and inexpensive method for determining the mechanical and transport properties of soil types, their distribution in space, and the type and distribution of the soil saturants (Campanella & Robertson, 1988; Mitchell & Brandon, 1998). In determining soil transport properties, the absolute magnitude or rate of decay of penetration-generated excess pore fluid pressures is correlated with the coefficient of consolidation of the soil and, via estimates of soil compressibility, with permeability.[1] (The term 'permeability' is used as a contraction for 'coefficient of permeability' throughout the following.) Current data reduction techniques may broadly be divided between methods that employ empirical correlations, and those that measure the generation or dissipation of pore fluid pressures, at the cone tip, face, or sleeve, either concurrent with penetration or after penetration-arrest. The latter include pump-type fluid injection tests.

Empirical predictions link recorded magnitudes of cone end-bearing, friction ratio and induced pore pressures with classifications of soils by grain size and type (Douglas & Olsen, 1981; Robertson *et al.*, 1986). These classifications may be used to estimate permeability coefficients directly from inferred soil type (Douglas & Olsen, 1981; Manassero, 1994), or may be further constrained by in situ imaging and the use of capillary models (Hryciw *et al.*, 2003). Alternative methods involve estimating coefficient of permeability directly from end-bearing (Chiang *et al.*, 1992; Smythe *et al.*, 1989) when sleeve friction is known.

Permeabilities may also be evaluated from uCPT-measured pore pressures. The coefficient of consolidation may be evaluated from dissipation rate following cone arrest, provided magnitudes of drained soil compressibility are also available. Several methods are used to calculate coefficient of consolidation (Levadoux & Baligh, 1986). All require that a pre-arrest pore pressure distribution may be determined. Most assume undrained loading for this evaluation, and incorporate cavity expansion (Torstensson, 1977; Burns & Mayne, 1998) or strain path models (Baligh, 1985; Baligh & Levadoux, 1986; Levadoux & Baligh, 1986; Teh & Houlsby, 1991; Danziger *et al.*, 1997) to define initial pore pressure distributions that may subsequently dissipate to background levels.

These evaluations compare well with field (Baligh & Levadoux, 1986; Levadoux & Baligh, 1986) and calibration chamber (Kurup *et al.*, 1994) results. Predictions of induced

strain fields and pore pressure magnitudes from complex (Baligh & Levadoux, 1986) and simple material models (Teh & Houlsby, 1991) compare well with more rigorous representations of finite strain continuum behaviour for clays (Kiousis & Voyiadjis, 1985; Voyiadjis & Abu-Farsakh, 1997; Voyiadjis & Song, 2000), sands (Cividini & Gioda, 1988) and clays to sands (Berg, 1994). For linear soil behaviour, a variant of these methods may be applied to account for partial drainage in an effective stress analysis (Elsworth, 1991, 1993, 1998), and this yields similar results to those from strain path and continuum models. Permeabilities are determined from consolidation coefficients via empirical estimates of soil compressibility. These estimates have a wide range, yielding estimates of permeability that exhibit a similar wide range (Lunne *et al.*, 1997). Other direct correlations of coefficient of consolidation with coefficient of permeability exist (Schmertmann, 1978) but are not broadly confirmed either by data (Robertson *et al.*, 1992), or on functional grounds.

For on-the-fly[†] evaluations (Elsworth, 1990; Elsworth & Lee, 2005), permeabilities are evaluated from the magnitudes of peak pore pressures recorded at the penetrometer tip.[‡] When pore pressures are generated around the cone tip and dissipate concurrently (as in sands), the behaviour may be viewed as a controlled strain-rate test. The magnitude of the steady pore fluid pressure is controlled by competition between the strain rate that generates excess pore pressure, and the permeability that dissipates it. Low permeabilities impede drainage and result in the generation of high excess pore pressures. The generation and concurrent dissipation of pore pressures around a blunt penetrometer may be represented by simple linear poroelastic models (Elsworth, 1990, 1991, 1992, 1993), but may also be evaluated using models representing the tapered form (Elsworth, 1998) of the tip and more realistic constitutive parameters (Song et al., 1999; Voyiadjis & Song, 2000; Voyiadjis & Song, 2003; Elsworth & Lee, 2004, 2005;).

Regardless of the method used, functional relations result that link permeability K with penetration rate U and excess pore pressure at the tip, $p - p_s$[4], relative to the static pore pressure magnitude p_s as $K \propto U/(p - p_s)$. (p is used to represent pore pressure magnitudes for consistency with prior publications, rather than the more conventional u.) This approach is attractive, because sounding is not interrupted to measure permeability, and the correlation with permeability is direct; no *a priori* measurement of soil compressibility is needed. However, a principal requirement in recovering permeabilities from peak pressure data is that penetration is partially drained; undrained measurements will provide information on soil strength and deformability only (Bai & Elsworth, 2000). In the following a rationale is first developed to discriminate between undrained and partially drained response, using cone metrics alone, and then methods are provided to recover permeability magnitudes from *bona fide* partially drained data. (Metrics are defined throughout as normalised magnitudes of end-bearing, sleeve frictional resistance, and induced pore fluid pressure.)

MECHANICAL RESPONSE

Permeability magnitudes may be recovered from tip-local pore pressure response only if the behaviour is partially

drained (Elsworth & Lee, 2005). Correspondingly, it is desired to discriminate between partially drained and undrained loading, using cone metrics, to determine regimes where permeability magnitudes may be confidently recovered.

Cone metrics

uCPT sounding yields profiles of cone resistance q_t, excess pore pressures, and sleeve friction f_s with depth. These dimensional metrics may be recast as normalised magnitudes of tip resistance Q_t, pore pressure ratio B_q and friction ratio F_r as

$$Q_t = \frac{q_t - \sigma_{v0}}{\sigma'_{v0}} \tag{1}$$

$$B_q = \frac{p - p_s}{q_t - \sigma_{v0}} \tag{2}$$

$$F_r = \frac{f_s}{q_t - \sigma_{v0}} \tag{3}$$

where σ_{v0} is the initial in situ vertical stress, p_s is the initial in situ pore pressure, and the prime denotes effective stress.

Cavity expansion solutions

For undrained loading, saturated soil appears to behave as a cohesive material, and this case is selected in the following. Limits may be placed on end-bearing and sleeve friction stresses, and on pore fluid pressures that may be developed during undrained penetration by considering cavity expansion solutions. Where a spherical cavity is expanded within an ideal elastic perfectly plastic soil ($c = S_u$; $\phi = 0$) from nominal radius to final radius a, with no net volume change at failure, as shown in Fig. 1, the resulting radial (σ_r) and tangential (σ_θ) stresses adjacent to the cavity wall are recorded as (Hill, 1983)

$$\sigma_r = \sigma_{v0} + \tfrac{4}{3}S_u[1 + \ln(G/S_u)] \tag{4}$$

$$\sigma_\theta = \sigma_{v0} + \tfrac{4}{3}S_u[1 + \ln(G/S_u)] - 2S_u \tag{5}$$

---

† The term 'on the fly' indicates that permeability is determined without the need for penetrometer arrest and determination through the monitoring of pore pressure dissipation, or for the use of *in situ* permeameters.

‡ Tip-measured pressures refer to those measured at the cone apex, on the face, or at the shoulder. For the spherical analysis discussed in the following, no distinction can be made between these locations.
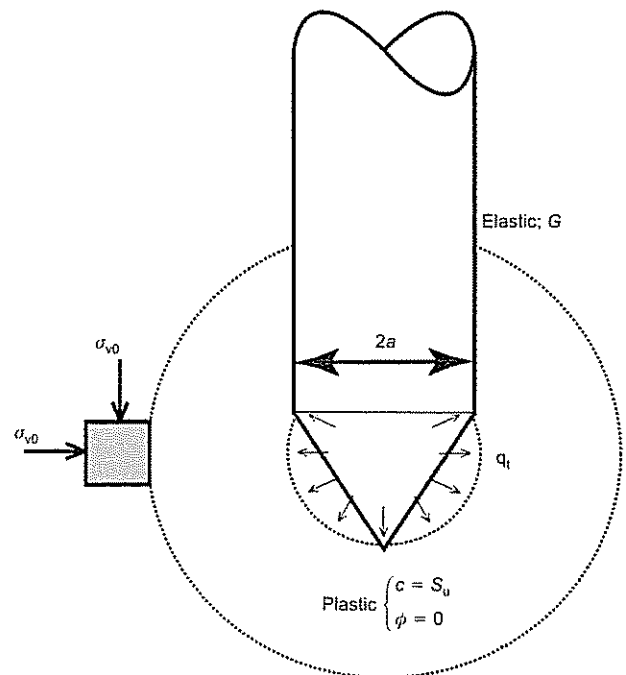

Fig. 1. Geometry for spherical expansion of a cavity of diameter $2a$ in a cohesive soil ($c = S_u$; $\phi = 0$) with uniform far-field total stress σ_{v0}.

where G is the shear modulus, and S_u is the undrained shear strength. These stresses are superposed on the initial pre-expansion total stress σ_{v0}, assumed uniform in vertical and horizontal directions. Cavity expansion stress q_t may be approximated by equation (4) as

$$q_t = \sigma_r = \sigma_{v0} + \tfrac{4}{3}S_u[1 + \ln(G/S_u)] \qquad (6)$$

although this typically acts as a lower bound to observations (Konrad & Law, 1987). The undrained pore pressures, $p - p_s$, generated during cavity expansion may be determined from the changes in mean total stress, $\Delta\sigma_m = \tfrac{1}{3}(\Delta\sigma_r + 2\Delta\sigma_\theta)$, and deviatoric total stress, $\Delta\sigma_d = \Delta\sigma_r - \Delta\sigma_\theta$, via the pore pressure relation $p - p_s = B\Delta\sigma_m + B\bar{A}\Delta\sigma_d$, where B and $\bar{A}$ are the pore pressure coefficients (Skempton, 1954). For saturated conditions it is assumed $B = 1$ and set $\bar{A}$ to zero, as a first assumption. From this, the excess pore pressure is recovered as

$$p - p_s = \tfrac{1}{3}(\Delta\sigma_r + 2\Delta\sigma_\theta) = \tfrac{4}{3}S_u\ln(G/S_u) \qquad (7)$$

representing the pressure induced and recorded at the cone tip. If the adhesion of the cone sleeve is assumed equal to the fully mobilised undrained shear strength, $f_s = S_u$, then the magnitudes of non-dimensional cone metrics of end-bearing, sleeve friction, and pore pressure ratio may be determined by substituting equations (6) and (7) into equations (1) to (3) to yield

$$B_q = \frac{p - p_s}{q_t - \sigma_{v0}} = \frac{\ln(G/S_u)}{1 + \ln(G/S_u)} \qquad (8)$$

$$Q_t = \frac{q_t - \sigma_{v0}}{\sigma_{v0}'} = \frac{4}{3}\frac{S_u}{\sigma_{v0}'}[1 + \ln(G/S_u)] \qquad (9)$$

$$F_r = \frac{f_s}{q_t - \sigma_{v0}} = \frac{1}{\tfrac{4}{3}[1 + \ln(G/S_u)]} \qquad (10)$$

These relations enable regions of undrained penetration to be denoted on plots of cone metrics typically used for soil classification, similar to Fig. 2. This figure defines a form of 'stress path,' shown schematically by the trajectory of point
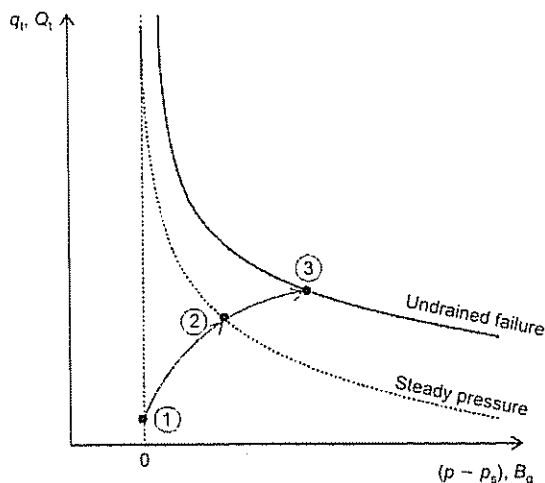

Fig. 2 Schematic plot of dimensional (q_t) or normalised (Q_t) tip resistance against excess pore pressure ($p - p_s$) or pore pressure ratio B_q, showing the stress path taken as penetration is initiated. Penetration initiates at 1 and may transit via 2 to undrained failure (3). If the material is granular, with relatively high permeability and high strength, penetration may be partially drained, resulting in the development of steady fluid pressure at the penetrometer tip (2)

1 to point 3 in Fig. 2. As penetration initiates at point 1, the tip resistance Q_t and pore pressure ratio B_q are limited by the 'failure envelope' at point 3. If the penetrated medium has a high permeability, undrained conditions may not be reached, and the resulting tip-local stress and pressure conditions will correspond to the dynamic steady state of point 2. This condition represents the condition of partial drainage where the rates of pore fluid pressure development and dissipation exactly cancel, enabling permeabilities to be evaluated from the peak pore pressure magnitude (Elsworth, 1993; Elsworth & Lee, 2005).

Where penetration is undrained, the resulting cone response is controlled by the strength of the soil alone, and generated pore pressures represent only this process, and provide no information on soil permeability. These relations may be determined for the usual plots of Q_t–B_q and Q_t–F_r, and the less commonly used plot of B_q–F_r, by combining equations (8) to (10) as

$$B_qQ_t = \frac{4}{3}\frac{S_u}{\sigma_{v0}'}\ln(G/S_u) \qquad (11)$$

$$Q_tF_r = \frac{S_u}{\sigma_{v0}'} \qquad (12)$$

$$\frac{B_q}{F_r} = \frac{4}{3}\ln(G/S_u) \qquad (13)$$

For typical magnitudes of $S_u/\sigma_{v0}' \approx 0\cdot3$ to $0\cdot7$ and $G/S_u \approx 20$ to 400, equations (11) to (13) yield bounds on the transition from undrained to partially drained behaviour as $B_qQ_t = 1\cdot2$ to $5\cdot6$, $Q_tF_r = 0\cdot3$ to $0\cdot7$, and $B_q/F_r = 4$ to 8. These bounds are illustrated in Fig. 3, isolating cone sounding metric products and ratios consistent with undrained behaviour, and by inference defining regions representing partially drained penetration.

These regions alone can be used to define whether permeability magnitudes may be evaluated from cone sounding metrics on the fly. Data are included that represent penetration under both presumed partially drained and undrained conditions; conformity to either of these modes is conditioned by the magnitudes of in situ permeability, reported in Table 1. Under standard penetration at 2 cm/s, the transition from partial drainage to undrained behaviour is expected to index directly with measured in situ permeability. Permeabilities decrease from the order of 10^{-3} to 10^{-5} m/s for sand and silts at Treasure Island, CA, and Savannah River, Aiken, SC, through silts of Tyrone, NM, to magnitudes of 10^{-9} m/s in varved clays at Amherst, MA. This transition in drainage condition is best honoured by the metrics of B_qQ_t and B_q/F_r apparent in Figs 3(a) and 3(c), exhibiting a sharp contrast between partially drained and undrained behaviour (partially drained = filled symbols; undrained = open symbols). This observation is confirmed by the statistics of the distribution. For the metric B_qQ_t, the threshold $B_qQ_t = 1\cdot2$ contains 85% of the 44 'partially drained' data points, and the threshold $B_qQ_t = 5\cdot6$ contains fully 96%, with only two outlying data points beyond the upper limit. Similarly, for B_q/F_r, the thresholds $B_q/F_r = 4$ and $B_q/F_r = 8$ contain successively 89% and 98% of the partially drained data points, with only a single outlier beyond the upper limit. These confirm the utility of these particular metrics in discriminating between drainage states.

Conversely, the metric Q_tF_r, shown in Fig. 3(b), is less definitive in defining the transition between drainage states. Although all the undrained data are restricted to the appropriate side of the most stringent threshold, at $Q_tF_r = 0\cdot7$ the partially drained data are distributed almost uniformly either side of the threshold. For this reason, this metric is not suitable as a discriminator of drainage state. This reflects the situation that neither normalised end-bearing nor normalised
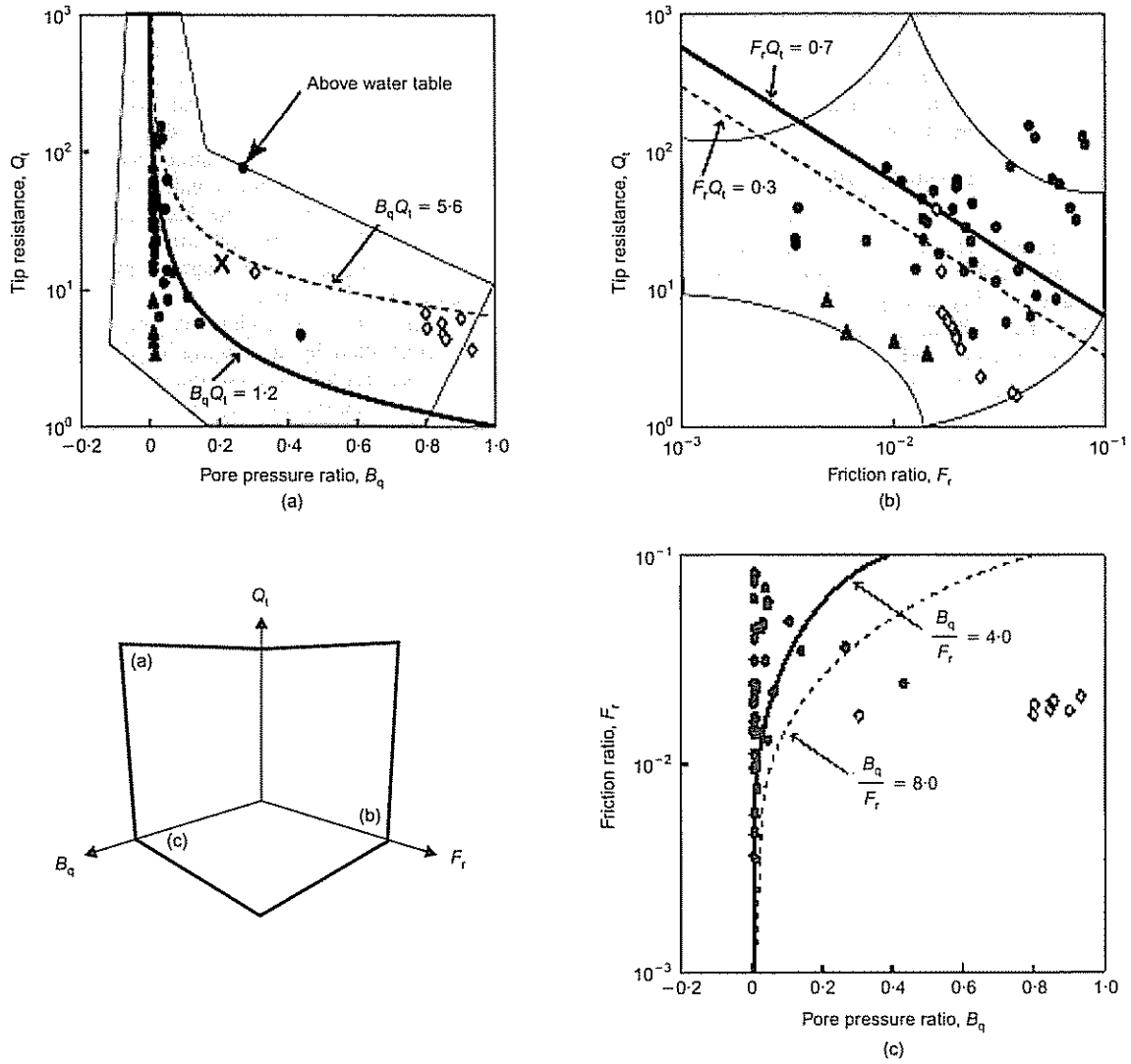
Fig. 3. Plots of cone metrics (a) $B_q Q_t$, (b) $Q_t F_r$ and (c) B_q/F_r with the range of threshold magnitudes defining the transition from partially drained to undrained behaviour (range of transition given by solid and dashed lines). Data are for a standard cone (10 cm²) advanced at standard rate (2 cm/s). Shaded regions in (a) and (b) denote defined ranges of material types (Robertson, 1990). Symbols denote data from varved clays at the NGES Amherst, MA, test site (diamonds), tailings slimes at Tyrone, NM (crosses), and sands and silts at Treasure Island, CA (triangles) and at the Savannah River test site, Aiken, SC (filled circles). Open symbols (crosses, diamonds) = undrained; filled symbols (triangles, circles) = partially drained. See Table 1 for details

Table 1. Permeability magnitudes reported for cone metric data reported in Figs 3 and 5

Location	Reported permeability: m/s	Soil characteristics	Presumed drainage characteristics	Source
Amherst, MA	3.0×10^{-9} to 4.0×10^{-9}	Normally consolidated varved clay	Undrained	DeGroot & Lutenegger (1994); Mayne, 2001
Tyrone, NM	1.0×10^{-8} to 7.4×10^{-8}	Silty clay	Undrained	Personal communication
Opelika, GA	3.5×10^{-7} to 1.5×10^{-6}	Residual silts and fine sands	Partially drained	Finke *et al.* (2001)
Savannah River, Aiken, SC	1.0×10^{-5} to 1.0×10^{-3}	Silts and sands	Partially drained	Personal communication
Treasure Island, CA	1.0×10^{-4} to 0.5×10^{-4}	Sand hydraulic fill	Partially drained	National geotechnical experimentation sites
Various	3.6×10^{-10} to 9.0×10^{-3}	Clay to sand	Partially drained to undrained	Voyiadjis & Song (2003)

sleeve friction, embodied in $Q_t F_r$, contains a direct measure of excess pore pressure—the most direct indicator of drainage state. Conversely, the metrics $B_q Q_t$ and B_q/F_r (represented in Figs 3(a) and 3(c)), each contain an intrinsic and

direct measure of excess pore pressure, via B_q. For these reasons, the use of $Q_t F_r$ is discouraged.

A final observation is that the boundaries between drained and undrained behaviour, apparent in Figs 3(a) and 3(b),

transect the soil facies types noted in related correlations (e.g. by Robertson, 1990). Notably, these observations are not contradictory, since although a single facies may have relatively tightly constrained mechanical attributes of strength, permeabilities may vary over multiple orders of magnitude. Since permeability therefore exerts the principal influence on the degree of drainage experienced under standard penetration, it is reasonable that one facies type could behave as either drained or undrained, depending primarily on the permeability. For this reason, practitioners are cautioned against using facies types as an indicator of drainage state, as the overriding influence of permeability transcends typical facies boundaries, as embodied in the relationship $B_q Q_t$ = constant relationship exhibited in Fig. 3(a).

PERMEABILITY FROM STEADY HYDRAULIC RESPONSE

With the limits defined that represent the transition from undrained to partially drained behaviour, it is possible to first isolate the data that conform to partial drainage, and to then use these data alone to determine permeability magnitudes. A relation is required that links in situ permeability magnitudes to measured steady tip pore pressures.

Hydraulic methods

Hydraulic methods require that a relation can be defined that links the tip-local permeability with the penetration-induced pore pressure. Assuming that the moving cone displaces a volume of fluid per unit time equivalent to the insertion volume of the cone, that this source dissipates roughly spherically, and that there is little fluid storage in the system, the induced pore pressures can be evaluated (Elsworth & Lee, 2004) as (Fig. 4)

$$\frac{p - p_s}{\sigma'_{v0}} = \frac{Ua\gamma_w}{4K\sigma'_{v0}} = \frac{1}{K_D} \tag{14}$$

where a is the penetrometer radius (synonymous with the cavity expansion radius defined earlier), and γ_w is the unit weight of water. These results are consistent with evaluations from dislocation methods (Elsworth, 1990). As apparent in

equation (14), permeability is related to a non-dimensional permeability, K_D. Noting that $(p - p_s)/\sigma'_{v0} = B_q Q_t$ (equations (1) and (2)) yields a single relation linking the cone metrics of end-bearing and pore pressure ratio as

$$K_D = 1/B_q Q_t \tag{15}$$

enabling permeability to be directly evaluated from cone metrics, provided they are recorded during partially drained penetrometer drivage.

Evaluation of available data

The permeability relation of equation (15) is applicable only where penetration is partially drained, with this threshold similarly defined uniquely in terms of $B_q Q_t$ by equation (11). Correspondingly, admissible cone data that are both partially drained, and for which permeability may therefore be evaluated from $K_D = 1/B_q Q_t$, are identified in Fig. 5. The same suite of data shown in Fig. 3 is included, together with additional data for which only composite magnitudes of the product $B_q Q_t$ are reported (Voyiadjis & Song, 2003). Again, the degree of drainage under standard penetration will be indexed to permeability, reported in Table 1. The threshold undrained behaviour is apparent for permeabilities lower than about 10^{-5} to 10^{-6} m/s ($K_D < 10^0$ to 10^{-1}), as reported earlier. This is signified by the plateau in $B_q Q_t$ data, in the range $10^0 < B_q Q_t < 10^1$. However, in addition, a preliminary correspondence is apparent between the data representing partial drainage and the relation $K_D = 1/B_q Q_t$ reported in equation (15), and also shown in the figure.

The utility of using a relationship of the general form $K_D = \alpha/(B_q Q_t)\beta$, where α and β are constants, is also shown in Fig. 5. This figure incorporates both the proposed limits to partially drained response (equation (11)), and appropriately defined permeability relations (equation (15)), defining
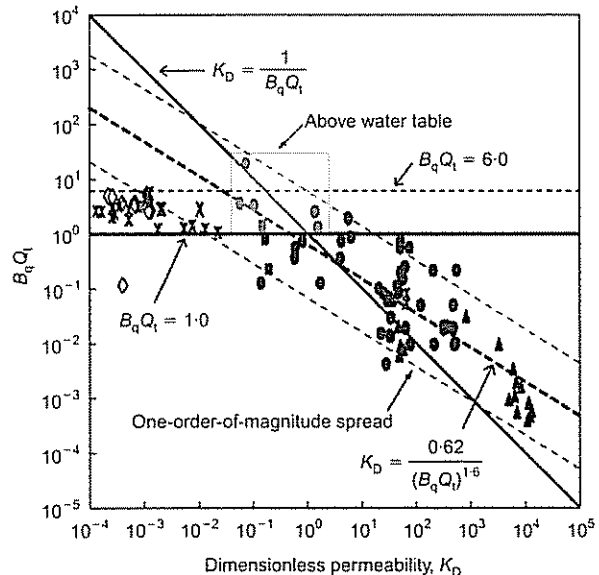
Fig. 5. Threshold magnitudes of excess pore pressure, $p - p_s/\sigma'_{v0} = B_q Q_t = 1/K_D$ relative to independently measured non-dimensional permeability K_D. The figure identifies both the transition from partially drained to undrained behaviour, and prospective relations for permeability, with data from the locations noted in Table 1. Amherst, MA (diamonds), Tyrone, NM (cross), Opelika, GA (squares), Savannah River, SC (circles), Treasure Island, CA (triangles), and Various (star). Open symbols (crosses, diamonds) = undrained; filled symbols (triangles, circles, squares) = partially drained; star = mixed. See Table 1 for details. Data are for a standard cone (10 cm²) advanced at standard rate (2 cm/s)
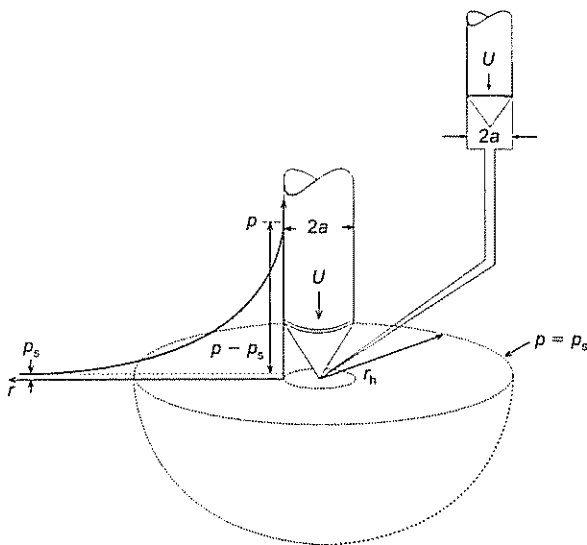

Fig. 4. Flow geometry local to the penetrometer tip. In partially drained penetration, the pore pressure is elevated at the centre of the spherical shell to p relative to the far-field pressure p_s, recorded at far-field radius r_h

non-dimensional permeability K_D. The transition from partially drained to undrained penetration is represented by the horizontal boundary. For the B_qQ_t metric, the presumed undrained data (Amherst, Tyrone, and various; Voyiadjis & Song, 2003) are most tightly constrained within the prescribed bounds of $1.2 < B_qQ_t < 5.6$. Usefully, non-dimensional permeabilities may be defined in terms of the same metric pairs that index the transition from partially drained to undrained behaviour. Where undrained data are ignored, the use of B_qQ_t shows a positive correspondence between the data and the proposed permeability relationship $K_D = 1/B_qQ_t$.

CONCLUSIONS

A methodology is developed that potentially enables permeability profiles to be recovered from cone metrics routinely recovered from uCPT soundings, on the fly. The technique requires that penetration be partially drained, resulting in the penetration-induced tip-local pore fluid pressures reflecting the competition between the penetration process that generates excess pressures, and the dissipation process that ameliorates them. The latter process, for the dynamic steady state that develops rapidly around the cone tip, is controlled primarily by the permeability of the surrounding soil, with the magnitude of the measured excess pore pressure therefore directly indexing permeability.

The proposed evaluation of permeability from the magnitude of peak pore fluid pressure requires that the penetration be partially drained, and that the pore pressure distribution has reached a dynamic steady state. The former is satisfied by excluding sounding data that are undrained, defined tentatively in this work as functions of the cone metric products and ratios B_qQ_t, Q_tF_r and B_q/F_r. The utility of these tentative metrics in identifying the transition between conditions of partial drainage and undrained behaviour, local to the cone tip, is confirmed by collocated sounding and permeability data in materials from clays to sands, and spanning the permeability range 10^{-9} to 10^{-3} m/s. Penetration at standard rate (2 cm/s), and with a standard cone (10 cm^2) represents a near-constant tip-local strain rate that generates tip pressures, and the transition to conditions of partial drainage should be indexed relative to permeability alone. This appears to be the case, with the transition identified for permeabilities of the order of 10^{-5} to 10^{-6} m/s, based jointly on characteristics of soil texture (Table 1), and on correspondence established between predicted and measured permeabilities (Fig. 5). For a larger-than-standard radius cone, or for faster-than-standard advance, the threshold permeability required to guarantee partially drained response will be raised. In addition, sounding intervals containing penetration-reduced (negative or sub-hydrostatic) pore pressures are excluded from the characterisation; these are not readily accommodated by the simple model presented here.

Where the penetration response is both partially drained and steady, permeability may be determined from the excess pore pressures through a relation of the form $K_D = \alpha/(B_qQ_t)^\beta$ for $B_qQ_t < 1.2$, where α and β are constants defined as unity from theory, and as $\alpha = 0.62$ and $\beta = 1.6$ from the fitting to observational data ($R^2 = 0.7$), and with a spread of approximately one order of magnitude either side of this relation. Although the currently available data are meagre, the reciprocal correlation between K_D and the metric pair B_qQ_t is clear. Related correlations of K_D with the alternative pairs Q_tF_r and B_q/F_r (not shown) are less promising and not independent: they are dependent both on the primary assumption that $K_D = 1/B_qQ_t$, and additionally on assumptions of tip local stresses that impart a further dependence on strength (in this case frictional strength). Correspondingly, a

relation of the form $K_D = \alpha/(B_qQ_t)^\beta$ with $B_qQ_t < 1.2$ is both the most fundamental and the most robust characterisation available. Importantly, permeabilities are recovered from sounding data recovered on the fly, without the need to arrest penetration or to either record pressure dissipation or conduct miniature pump tests through the injection or recovery of fluids through the tip. Correspondingly, this method may be applied *a posteriori* to the extensive worldwide archive of sounding data, enabling permeability profiles to be recovered where these data were initially neither recovered, nor sought.

ACKNOWLEDGEMENTS

NOTATION

a	penetrometer radius; L
B_q	dimensionless pore pressure ratio, $(p - p_s)/(q_t - \sigma_{v0})$
c	cohesion; FL^{-2}
F_r	normalized friction factor, $f_s/(q_t - \sigma_{vo})$
f_s	magnitude of sleeve friction; FL^{-2}
G	shear modulus; FL^{-2}
K	permeability (coefficient of permeability); LT^{-1}
K_D	dimensionless hydraulic conductivity, $(4K\sigma_{v0})/(Ua\gamma_w)$
p	absolute pore fluid pressure (u_2); FL^{-2}
p_s	initial static fluid pressure; FL^{-2}
$p - p_s$	excess pore pressure; FL^{-2}
Q_t	normalized cone resistance, $(q_t - \sigma_{v0})/\sigma_{v0}$
q_c	measured cone resistance; FL^{-2}
q_t	corrected cone resistance, $q_c + (1 - a_n)p$; FL^{-2}
S_u	undrained shear strength; FL^{-2}
U	penetrometer penetration rate; LT^{-1}
γ_w	unit weight of water; FL^{-3}
σ_r	radial stress; FL^{-2}
σ_θ	tangential stress; FL^{-2}
σ_v	total vertical stress; FL^{-2}
$\sigma_{v0}, \sigma'_{v0}$	initial vertical stress and effective stress; FL^{-2}
ϕ	friction angle

REFERENCES

Bai, M. & Elsworth, D. (2000). *Coupled processes in subsurface deformation, flow, and transport*. Reston, VA: ASCE Press.

Baligh, M. M. (1985). Strain path method. *J. Geotech. Engng* **111**, No. 9, 1108–1136.

Baligh, M. M. & Levadoux, J. N. (1986). Consolidation after undrained piezocone penetration. II: Interpretation. *J. Geotech. Engng* **112**, No. 7, 727–745.

Berg, V. D. (1994). *Analysis of soil penetration*. PhD thesis, Delft University, Netherlands.

Burns, S. E. & Mayne, P. W. (1998). Monotonic and dilatory pressure decay during piezocone tests in clay. *Can. Geotech. J.* **35**, No. 6, 1063–1073.

Campanella, R. G. & Robertson, P. K. (1988) Current status of the piezocone test. *Proc. Penetration Testing 1988, Orlando*, 93–116.

Chiang, C. Y., Loos, K. R. & Klopp, R. A. (1992). Field determination of geological/chemical properties of an aquifer by cone penetrometry and head-space analysis. *Ground Water* **30**, No. 3, 428–436.

Cividini, A. & Gioda, G. (1988). A simplified analysis of pile penetration. *Proc. 6th Int. Conf. Numer. Methods Geomech., Innsbruck*, 1043–1049.

Danziger, F. A. B., Almeida, M. S. S. & Sills, G. C. (1997). The significance of the strain path analysis in the interpretation of piezocone dissipation data. *Géotechnique* **47**, No. 5, 901–914.

DeGroot, D. J. & Lutenegger, A. J. (1994). A comparison between field and lab measurements of hydraulic conductivity in a varved clay. In *Hydraulic conductivity and waste contaminant transport*

in soil, STP 1142, pp. 300–317. West Conshohocken, PA: ASTM International.

Douglas, B. J. & Olsen, R. S. (1981) Soil classification using electric cone penetrometer. *Proceedings of the symposium on cone penetration testing and experience*, St Louis, pp. 209–227.

Elsworth, D. (1990). Theory of partially drained piezometer insertion. *J. Geotech. Engng* 116, No. 6, 899–914.

Elsworth, D. (1991). Dislocation analysis of penetration in saturated porous media. *J. Engng Mech.* 117, No. 2, 391–408.

Elsworth, D. (1992). Pore pressure response due to penetration through layered media. *Int. J. Numer. Anal. Methods Geomech.* 16, No. 1, 45–64.

Elsworth, D. (1993). Analysis of piezocone dissipation data using dislocation methods. *J. Geotech. Engng* 119, No. 10, 1601–1623.

Elsworth, D. (1998). Indentation of a sharp penetrometer in a poroelastic medium. *Int. J. Solids Struct.* 35, No. 34–35, 4895–4904.

Elsworth, D. & Lee, D. S. (2005). Permeability determination from on-the-fly piezocone sounding. *J. Geotech. Geoenviron. Engng* 131, No. 5, 643–653.

Finke, K. A., Mayne, P. W. & Klopp, R. A. (2001). Piezocone penetration testing in Atlantic piedmont residuum. *J. Geotech. Geoenviron. Engng* 127, No. 1, 48–54.

Hill, R. (1983). *The mathematical theory of plasticity*. Oxford: Oxford University Press.

Hryciw, R. D., Shin, S. & Ghalib, A. M. (2003). High resolution site characterization by visCPT with application to hydrogeology.' *Proc. 12th Panamerican Conf. Soil Mech., Boston*, 293–298.

Kiousis, P. D. & Voyiadjis, G. Z. (1985). Lagrangian continuum theory for saturated porous media. *J. Engng Mech.* 111, No. 10, 1277–1288.

Konrad, J. M. & Law, K. T. (1987). Undrained shear-strength from piezocone tests. *Can. Geotech. J.* 24, No. 3, 392–405.

Kurup, P. U., Voyiadjis, G. Z. & Tumay, M. T. (1994). Calibration chamber studies of piezocone tests in cohesive soils. *J. Geotech. Engng* 120, No. 1, 81–107.

Levadoux, J. N. & Baligh, M. M. (1986). Consolidation after undrained piezocone penetration. I: Prediction. *J. Geotech. Engng* 112, No. 7, 707–725.

Lunne, T., Robertson, P. K. & Powell, J. J. M. (1997). *Cone penetration testing in geotechnical practice*. London: Blackie Academic.

Manassero, M. (1994). Hydraulic conductivity assessment of slurry wall using piezocone test. *J. Geotech. Engng* 120, No. 10, 1725–1746.

Mayne, P. W. (2001). Stress-strain-strength-flow parameters from enhanced in-situ tests. *Proceedings of the international conference on in-situ measurement of soil properties and case histories (In-Situ 2001)*, Bali, pp. 27–48.

Mitchell, J. K. & Brandon, T. L. (1998). Analysis and use of CPT in earthquake and environmental engineering. *Geotechnical Site Characterization*. Rotterdam: Balkema, 1, 69–96.

Robertson, P. K. (1990). Soil classification using the cone penetration test. *Can. Geotech. J.* 27, No. 1, 151–158.

Robertson, P. K., Campanella, R. G., Gillespie, D. & Greig, J. (1986). Use of piezometer cone data. *Proc. ASCE Spec. Conf. In Situ '86. Use of In Situ Tests in Geotechnical Engineering, Blacksburg*, 1263–1280.

Robertson, P. K., Sully, J. P., Woeller, D. J., Lunne, T., Powell, J. J. M. & Gillespie, D. G. (1992). Estimating coefficient of consolidation from piezocone tests. *Can. Geotech. J.* 29, No. 4, 539–550.

Schmertmann, J. H. (1978). *Guidelines for cone penetration test: Performance and design*. Federal Highway Administration Report No. FHWA-TS-78-209. Washington, DC: US Dept of Transportation.

Skempton, A. W. (1954). The pore pressure coefficients A and B. *Géotechnique* 4, No. 4, 143–147.

Smythe, J. M., Bedient, P. B., Klopp, R. A. & Chiang, C. Y. (1989) An advanced technology for the in situ measurement of heterogeneous aquifers. *Proceedings of the conference New Field Tech. Quant. Phys. Chem. Prop. Heter. Aquifers*, Dallas, pp. 605–628.

Song, C. R., Voyiadjis, V. G. & Tumay, M. T. (1999). 'Determination of permeability of soils using the multiple piezo-element penetrometer. *Int. J. Numer. Anal. Methods Geomech.* 23, No. 13, 1609–1629.

Teh, C. & Houlsby, G. (1991). An analytical study of the cone penetration test in clay. *Géotechnique* 41, No. 1, 17–34.

Torstensson, B. A. (1977). The pore pressure probe. *Nordiske Geotekniske Mote* 34, No. 34, 1·34·15.

Voyiadjis, G. Z. & Abu-Farsakh, M. Y. (1997). Coupled theory of mixtures for clayey soils. *Comput. Geotech.* 20, No. 3/4, 195–222.

Voyiadjis, G. Z. & Song, C. R. (2000). Finite strain anisotropic Cam Clay model with plastic spin. II: Application to piezocone test. *J. Engng Mech.* 126, No. 10, 1020–1026.

Voyiadjis, G. Z. & Song, C. R. (2003). Determination of hydraulic conductivity using piezocone penetration test. *Int. J. Geomech.* 3, No. 2, 217–224.